An *in vivo* ESR spin-trapping study: Free radical generation in rats from formate intoxication—role of the Fenton reaction

Anna E. Dikalova, Maria B. Kadiiska, and Ronald P. Mason*

Laboratory of Pharmacology and Chemistry, National Institute of Environmental Health Sciences, National Institutes of Health, Research Triangle Park, NC 27709

Edited by Helmut Beinert, University of Wisconsin, Madison, WI, and approved September 20, 2001 (received for review February 22, 2001)

Electron spin resonance spectroscopy has been used to study free radical generation in rats with acute sodium formate poisoning. The *in vivo* spin-trapping technique was used with α-(4-pyridyl-1-oxide)-*N*-*t*-butylnitrone (POBN), which reacts with free radical metabolites to form radical adducts, which were detected in the bile and urine samples from Fischer rats. The use of [^{13}C]-sodium formate and computer simulations of the spectra identified the 12-line spectrum as arising from the POBN/carbon dioxide anion radical adduct. The identification of POBN/$^{\cdot}CO_2^-$ radical adduct provides direct electron spin resonance spectroscopy evidence for the formation of $^{\cdot}CO_2^-$ radicals during acute intoxication by sodium formate, suggesting a free radical metabolic pathway. To study the mechanism of free radical generation by formate, we tested several known inhibitors. Both allopurinol, an inhibitor of xanthine oxidase, and aminobenzotriazole, a cytochrome P450 inhibitor, decreased free radical formation from formate, which may imply a dependence on hydrogen peroxide. In accord with this hypothesis, the catalase inhibitor 3-aminotriazole caused a significant increase in free radical formation. The iron chelator Desferal decreased the formation of free radicals up to 2-fold. Presumably, iron plays a role in the mechanism of free radical generation by formate via the Fenton reaction. The detection of formate free radical metabolites generated *in vivo* and the key role of the Fenton reaction in this process may be important for understanding the pathogenesis of both formate and methanol intoxication.

Formic acid is a common metabolic intermediate in living cells. However, in high doses, it is very toxic. The toxicology of formic acid has been investigated mainly in connection with methanol studies (1–3). There are no recent reviews on formic acid itself, although it is commonly used in the modern chemical industry (1).

Exposure to formic acid leads to its accumulation in the body. The maximum concentration of formic acid measured in rabbit blood, brain, heart, liver, and kidney after five daily i.v. doses was similar to that causing impaired oxidative metabolism and damage at the cellular level (4). The optic nerve and other organs (brain, heart, and kidneys) with a high rate of oxygen consumption are possible targets (5). Formate accumulation is the principal, if not the only, reason for the development of acidosis, which is usually observed after methanol poisoning (6, 7). Acidosis may cause the inhibition of cellular respiration and hasten the onset of cellular injury. Also, progressive acidosis will induce circulatory failure, leading to tissue hypoxia and lactic acid production, both of which further increase the acid load, in turn increasing undissociated formic acid. This cycle is called "circulus hypoxicus" (8).

Formic acid and methanol have common mechanisms of toxicity, because formic acid is a metabolic end product of methanol and is mainly responsible for the toxic inhibition of cytochrome *c* oxidase. Inhibition of the cytochrome *c* oxidase complex leads to anaerobic glycolysis and lactic acidosis—"histotoxic hypoxia" (9). It was hypothesized that because of acidosis, the generation of oxygen radicals might be enhanced, leading to membrane damage, lipid peroxidation, and mitochondrial damage (10, 11).

The aim of this work was to apply the electron spin resonance spectroscopy (ESR) spin-trapping technique to the detection of free radical metabolites generated during acute formate poisoning and to find possible mechanisms of their generation.

Materials and Methods

α-(4-pyridyl-1-oxide)-*N*-*t*-butylnitrone (POBN) was obtained from Alexis (San Francisco, CA) and Sigma. Sodium formate, 2,2′-dipyridyl (DP), bathocuproinedisulfonic acid disodium salt hydrate (BC), allopurinol, 1-aminobenzotriazole (ABT), deferoxamine mesylate, 4-hydroxyl-tempo, Desferal and peroxidase were all obtained from Sigma. Sodium formate (99 atom % ^{13}C), gadolinium (III) chloride hexahydrate, and 3-amino-1,2,4-triazole (AT) were obtained from Aldrich. Dimethyl-^{13}C sulfoxide ([$^{13}C_2$]-DMSO) was obtained from Isotec. Superoxide dismutase (SOD) and catalase were obtained from Boehringer Mannheim.

Fischer male rats (300–400 g) (Charles River Breeding Laboratories) were used in all experiments. Rats were fed a standard chow mix (NIH open formula, Ziegler Brothers, Gardner, PA). Nonfasted rats were anesthetized by an i.p. injection of 50 mg/kg body weight of Nembutal. Bile was collected by bile duct cannulation via a segment of PE-10 tubing (Becton Dickinson).

***In Vivo* Studies.** Bile samples (300 μl) were collected every 20 min for 2 h into plastic Eppendorf tubes containing a 50-μl solution of DP (30 mM) and BC (30 mM) (12). The samples were frozen in dry ice immediately after collection and stored at −70°C until ESR analysis was performed.

Both POBN and sodium formate were dissolved separately in HPLC grade water (Merck) and injected simultaneously i.p. at 1.5 g/kg and 2 g/kg body weight, respectively.

In other studies, ABT (100 mg/kg, i.p.) (13) or gadolinium chloride ($GdCl_3$, 10 mg/kg, i.v.) (14) in saline was administered to rats 2 or 24 h, respectively, before the administration of sodium formate and the spin trap. Where indicated, rats were injected i.p. with Desferal (50 mg/kg) 1 h before the injection of POBN and sodium formate (15). Allopurinol was administered to rats i.p. (50 mg/kg), 24 and 5 h before the injection of sodium formate and POBN (16). AT was given to rats (1 g/kg, i.p.) 1 h

This paper was submitted directly (Track II) to the PNAS office.

Abbreviations: ESR, electron spin resonance spectroscopy; POBN, α-(4-pyridyl-1-oxide)-*N*-*t*-butylnitrone; DP, 2,2′-dipyridyl; BC, bathocuproinedisulfonic acid disodium salt hydrate; ABT, aminobenzotriazole; AT, 3-amino-1,2,4-triazole; SOD, superoxide dismutase; THF, tetrahydrofolate.

*To whom reprint requests should be addressed at: Laboratory of Pharmacology and Chemistry, National Institute of Environmental Health Sciences, 111 Alexander Drive, P.O. Box 12233, Mail Drop F-01, Research Triangle Park, NC 27709. E-mail: Mason4@niehs.nih.gov.

The publication costs of this article were defrayed in part by page charge payment. This article must therefore be hereby marked "*advertisement*" in accordance with 18 U.S.C. §1734 solely to indicate this fact.

before sodium formate administration (17, 18). DMSO was injected (2 ml/kg, i.p.) 1 h before sodium formate and POBN administration.

Urine samples (300 μl) were collected from the bladder into a 50-μl solution of the chelators DP (30 mM) and BC (30 mM) 1 and 2 h after the injection of sodium formate and the spin-trap POBN. The samples were frozen in dry ice immediately after collection and stored at −70°C until ESR analysis was performed.

The animal protocol we used was approved by the National Institute of Environmental Health Sciences Animal Care and Use Committee, and all animals received humane care in compliance with the National Research Council's criteria for humane care as outlined in the Guide for the Care and Use of Laboratory Animals prepared by the National Academy of Sciences and published by National Institutes of Health (19).

***In Vitro* Studies.** POBN (20 mM) and 100 mM sodium formate were added to the bile or urine containing 5 mM DP and 5 mM BC. [^{13}C]-sodium formate (10 mM), 100 mM POBN, and 10 mM H_2O_2 were mixed in the collecting tube, and the ESR spectrum was recorded. The same experiment was repeated with the addition of horseradish peroxidase (100 units/ml) or catalase (6,500 units/ml). All *in vitro* experiments were done in triplicate.

ESR Measurements. ESR spectra were recorded on an EMX spectrometer equipped with a Super High Q cavity (Bruker, Billerica, MA). The ESR settings and experimental conditions are indicated in the figure legends. Hyperfine coupling constants were determined by using a spectral simulation program (20).

Concentration of POBN Radical Metabolites: Calculation. ESR spectra of bile samples were recorded, and POBN radical adduct concentrations were determined by double integration of their respective spectra. 4-Hydroxyl-tempo (TEMPO-OH) solution (77.4 μM) was used as a concentration standard, and all required conditions applied to both standard and experimental samples were followed (21). The TEMPO-OH concentration was determined by using an extinction coefficient at 242 nm of 2,915 $M^{-1}\cdot cm^{-1}$ (22).

Statistical Analysis. Data were expressed as mean ± SEM. Statistical significance between groups was determined by the analysis of variance and Student's t test. Differences were considered significant when $P < 0.05$.

Results

A strong six-line ESR signal of the POBN radical adduct was detected in the bile of rats after acute sodium formate poisoning (Fig. 1*A*). The hyperfine coupling constants for this radical adduct (a^N = 15.54 G and a^H_β = 3.46 G) corresponded to those determined previously for POBN/$^{\cdot}CO_2^-$ (23). The additional small doublet signal in this spectrum, often detected in bile samples, is from the ascorbate semidione radical. When the experiment was repeated without sodium formate administration, only a residual signal of POBN radical adducts was observed (Fig. 1*B*), confirming the formate dependence of the radical adduct shown in Fig. 1*A*. The six-line spectrum is characteristic of many free radicals trapped by POBN. The hyperfine coupling constants of the radical adduct in Fig. 1*B* (a^N = 15.55 G and a^H_β = 3.10 G) are not definitive but could be those of carbon-centered endogenous radicals, perhaps lipid-derived (24). Only the ESR signal of the ascorbate semidione radical was detected in bile when sodium formate was injected into the rat without POBN (Fig. 1*C*).

To identify the detected radical adduct, experiments were performed by using [^{13}C]-sodium formate (Fig. 1*D*). The computer simulation of the spectrum (Fig. 1*E*) showed that it

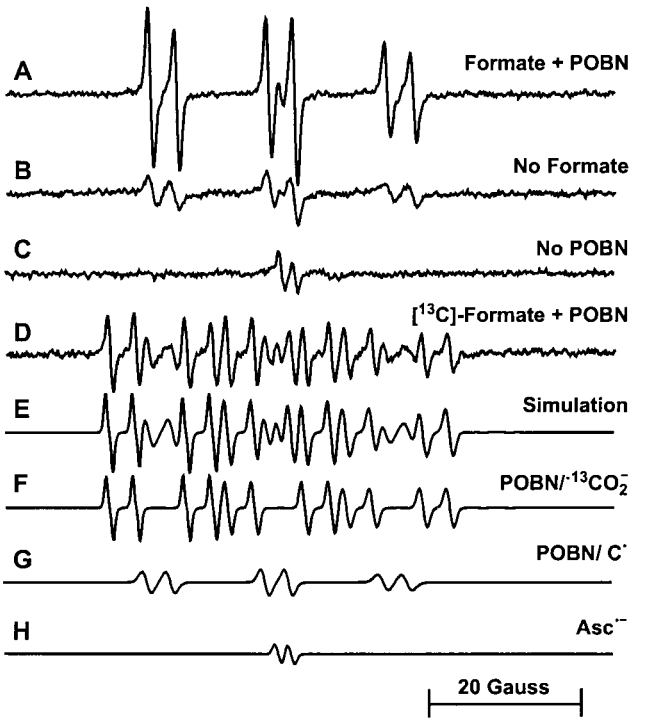

Fig. 1. Spectrum A: ESR spectrum of radical adducts detected in bile of rats 1 h after acute sodium formate (2 g/kg) and POBN (1.5 g/kg) i.p. administration. Spectrum B: same as A, except without sodium formate administration. Spectrum C: same as A, except without POBN administration. Spectrum D: ESR spectrum in bile of rats 1 h after acute [^{13}C]-sodium formate (2 g/kg) and POBN (1.5 g/kg) i.p. administration. Spectrum E: composite computer simulation of the spectrum in *D*. Spectrum F: 12-line computer simulation of the POBN/$^{\cdot 13}CO_2^-$ radical adduct (63–65%). Spectrum G: computer simulation of the spectrum from unknown POBN/carbon-centered radicals (29–31%). Spectrum H: computer simulation of the spectrum from the ascorbate semidione radical, $Asc^{\cdot -}$ (6–7%). Instrumental settings of Bruker EMX spectrometer: microwave power, 20 mW; modulation amplitude, 1 G; scan time 660 s; time constant, 1.3 s, and a single scan of 80 G.

contained three radical species. The hyperfine coupling constants of the predominant species (63–65% of the radical adducts) were a^N = 15.56 ± 0.10 G, a^H_β = 3.49 ± 0.08 G and a^{13C}_β = 10.15 ± 0.09 G (n = 4) (Fig. 1*F*). The presence of the [^{13}C] hyperfine coupling confirmed that this radical adduct was derived from sodium formate, and we assigned it as the POBN/$^{\cdot 13}CO_2^-$ radical adduct (23). The hyperfine coupling constants of the second radical species (Fig. 1*G*) were a^N = 15.91 ± 0.07 G and a^H_β = 3.19 ± 0.05 G (n = 4), corresponding to a carbon-centered endogenous radical of unknown origin. The third radical adduct was the ascorbate-derived semidione radical with a coupling constant of a^H_β = 1.67 ± 0.02 G (n = 4) (Fig. 1*H*).

Further evidence for the *in vivo* radical generation by formate was provided with the following control experiments. Rats were injected with POBN (1.5 g/kg), and bile was collected into an Eppendorf tube containing sodium formate (100 mM), DP (5 mM), and BC (5 mM). Only a minor signal was detected by ESR (Fig. 2*B*), thus confirming that the spectra shown in Figs. 1*A* and 2*A* were from radical adducts formed *in vivo*. Likewise, if sodium formate was administered *in vivo*, but POBN (20 mM) was added to the collecting tube with the chelators DP and BC, again, no signal was detected (Fig. 2*C*). When both POBN (20 mM) and sodium formate (100 mM) were mixed in the collecting tube with bile in the presence of DP (5 mM) and BC (5 mM), only a minor residual signal of POBN radical adduct was observed (Fig. 2*D*).

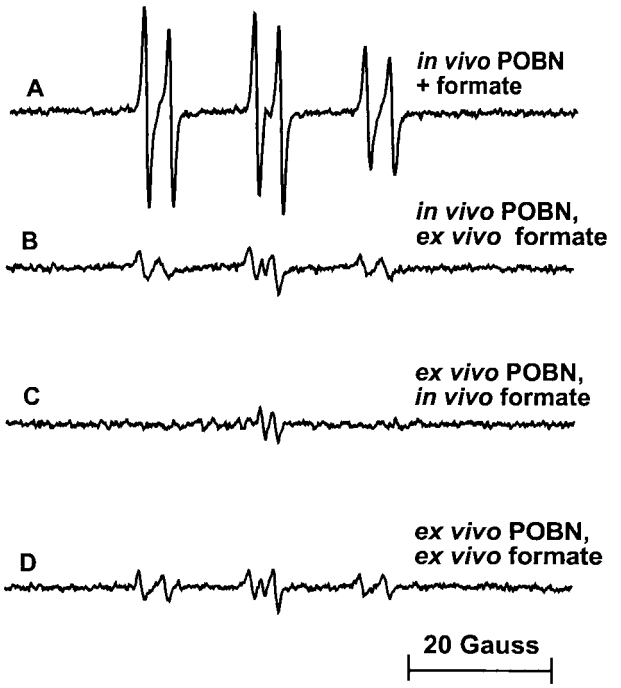

Fig. 2. Spectrum A: ESR spectrum of radical adducts detected in bile of rats 1 h after acute sodium formate (2 g/kg) and POBN (1.5 g/kg) i.p. administration. Spectrum B: same as A, except sodium formate (100 mM) was added *ex vivo* to the collection tube instead of being administered *in vivo*. Spectrum C: same as A, except sodium formate was administered *in vivo*, whereas 20 mM POBN was added to the collection tube *ex vivo*. Spectrum D: same as A, except both formate (100 mM) and POBN (20 mM) were added to the collection tube *ex vivo*. Instrumental settings of Bruker EMX spectrometer: microwave power, 20 mW; modulation amplitude, 1 G; scan time, 660 s; time constant, 1.3 s, and a single scan of 80 G.

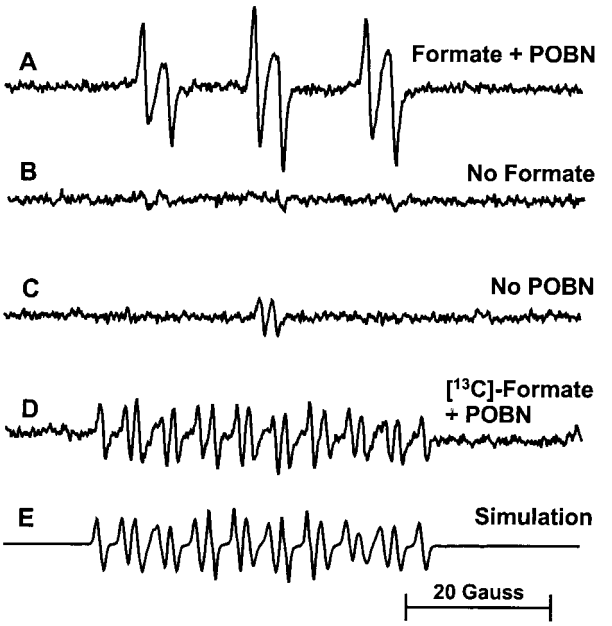

Fig. 3. Spectrum A: ESR spectrum of radical adducts detected in urine of rats 1 h after acute sodium formate (2 g/kg) and POBN (1.5 g/kg) i.p. administration. Spectrum B: same as A, but without sodium formate administration. Spectrum C: same as A, but without POBN administration. Spectrum D: ESR spectrum of radical adducts detected in urine of rats 1 h after acute [^{13}C]-sodium formate (2 g/kg) and POBN (1.5 g/kg) i.p. administration. Spectrum E: computer simulation of the spectrum in A. Instrumental settings of Bruker EMX spectrometer: microwave power, 20 mW; modulation amplitude, 1 G; scan time, 660 s; time constant, 1.3 s, and a single scan of 80 G.

To exclude an *ex vivo* Fenton chemical reaction, we repeated the experiments with SOD and catalase present in the collecting tube. Bile from rats injected with sodium formate and a spin trap was collected into a tube containing SOD (5,000 units/ml) or catalase (1 mg/ml). There was no effect from either SOD or catalase on the amplitude of the ESR signal (data not shown).

In addition, *in vitro* experiments were performed in which 10 mM [^{13}C]-sodium formate, 100 mM POBN, and 10 mM H_2O_2 were mixed in the collecting tube. No signal from the POBN/$^{\bullet 13}CO_2^-$ radical adduct was detected. Neither was this radical adduct detected when the experiment was repeated with the addition of horseradish peroxidase (100 units/ml) or catalase (6,500 units/ml) (data not shown). This result excludes the possibility that formate is oxidized to the carbon dioxide anion radical by peroxidase or the peroxidase activity of catalase.

A six-line ESR signal was also detected in the urine 1 h after i.p. injection of sodium formate and POBN (Fig. 3*A*). When the experiment was repeated without sodium formate administration, only a minor residual signal of POBN radical adduct was observed (Fig. 3*B*), demonstrating that the radical adduct was formate-dependent. No six-line ESR signal was detected in urine when only sodium formate was injected into the rat without the spin trap (Fig. 3*C*). It was found that the ESR signal was weaker 2 h after the administration of sodium formate and POBN, and after 3 h, it had completely disappeared (data not shown). The experiment with [^{13}C]-sodium formate revealed a 12-line spectrum component (Fig. 3*D*). Computer simulations of the spectra showed that hyperfine coupling constants for the three radical species used for simulation of POBN radical adducts in urine were exactly the same as the ones in bile (Fig. 3*E*). The predominant species was the POBN/$^{\bullet 13}CO_2^-$ radical adduct.

To study the mechanism of free radical generation by formate, we tested several known enzyme inhibitors, which were administered to the rats before treatment with formate and POBN (Fig. 4).

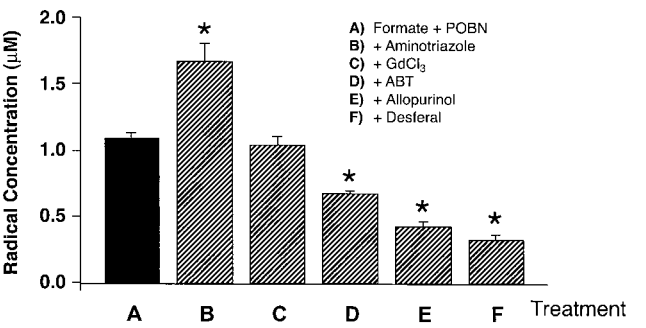

Fig. 4. Column A: POBN/$^{\bullet}CO_2^-$ radical adduct concentration (μM) in bile 1 h after injection of sodium formate (2 g/kg, i.p.) and POBN (1.5 g/kg, i.p.). Column B: same as A, but rats were pretreated with aminotriazole (2 g/kg, i.p.) 1 h before sodium formate injection. Column C: same as A, but the rats were pretreated with gadolinium chloride (10 mg/kg, i.v.) 24 h before the injection of sodium formate and POBN. Column D: same as A, but rats were pretreated with aminobenzotriazole (100 mg/kg, i.p.) 2 h before sodium formate and POBN administration. Column E: same as A, but rats were pretreated twice with allopurinol (100 mg/kg) 24 and 5 h before sodium formate and POBN administration. Column F: same as A, but rats were pretreated with Desferal (50 mg/kg) 1 h before sodium formate and POBN administration. Values are the mean ± SEM of $n = 10$. Asterisks indicate statistically significant ($P < 0.05$) compared with *A*.

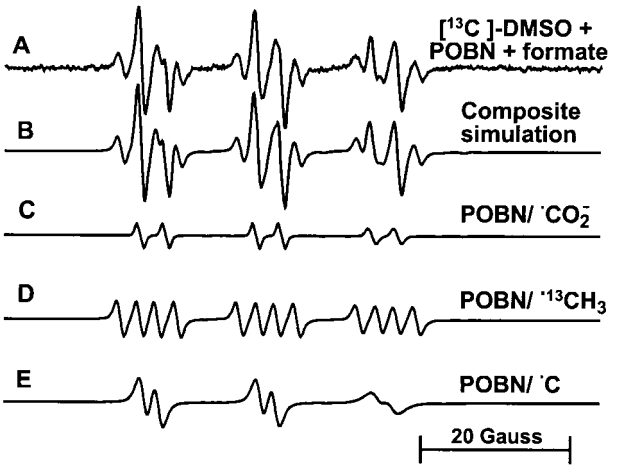

Fig. 5. Spectrum A: ESR spectrum of radical adducts detected in bile of rats 2 h after [$^{13}C_2$]-DMSO injection (1 g/kg, i.p.) followed after 1 h by sodium formate (2 g/kg) and POBN (1.5 g/kg) i.p. administration. Spectrum B: composite computer simulation of the spectrum in A. Spectrum C: six-line computer-simulated spectrum of the POBN/$^{\cdot}CO_2^-$ radical adduct (23–24%). Spectrum D: computer simulation of the spectrum of the POBN/$^{\cdot}{}^{13}CH_3$ adduct (35–36%). Spectrum E: computer simulation of the spectrum from POBN/carbon-centered radicals (39–40%). Instrumental settings of Bruker EMX spectrometer: microwave power, 20 mW; modulation amplitude, 1 G; scan time, 660 s; time constant, 1.3 s, and a single scan of 80 G.

Pretreatment with the catalase inhibitor AT (1 g/kg) 1 h before administration of formate and the spin trap showed a significant increase in free radical generation (Fig. 4*B*), as compared with the group treated only with formate and POBN (Fig. 4*A*).

Gadolinium chloride, an inhibitor of Kupffer cells, administered i.v. (10 mg/kg) 24 h before formate and POBN injection, was not found to cause any significant changes in radical production compared with formate alone (Fig. 4*C*).

Rats pretreated with ABT (100 mg/kg, i.p.), a suicide substrate of cytochrome P450s, had significantly lower levels of free radical generation after sodium formate administration (Fig. 4*D*).

Allopurinol (100 mg/kg, i.p.), an inhibitor of xanthine oxidase given 24 and 5 h before the injection of sodium formate and POBN, also caused a statistically significant decrease of free radical generation (Fig. 4*E*).

Interestingly, when Desferal (50 mg/kg, i.p.) was given 1 h before the administration of sodium formate and POBN, a statistically significant decrease in the formation of free radicals was found (Fig. 4*F*). In addition, treatment with DMSO (2 ml/kg, i.p.) 1 h before sodium formate and POBN administration resulted in a markedly decreased intensity of the POBN/$^{\cdot}CO_2^-$ signal when compared with the signal detected from rats given only formate and POBN (data not shown). When [$^{13}C_2$]-DMSO was injected into a rat 1 h before sodium formate and POBN administration, a 12-line ESR spectrum was obtained (Fig. 5*A*). Composite simulation of the spectrum (Fig. 1*B*) showed the presence of two identifiable radical species: POBN/$^{\cdot}CO_2^-$, with coupling constants $a^N = 15.55 \pm 0.04$ G and $a_\beta^H = 3.43 \pm 0.02$ G (Fig. 1*C*), and POBN/$^{\cdot}CH_3$ (25), with coupling constants $a^N = 16.04 \pm 0.02$ G, $a_\beta^H = 2.65 \pm 0.03$ G, and $a_\beta^{13C} = 5.03 \pm 0.01$ G (Fig. 1*D*). The third radical species used for simulation has the following coupling constants: $a^N = 15.67 \pm 0.03$ G and $a_\beta^H = 1.99 \pm 0.02$ G (Fig. 1*E*). The concentration of POBN/$^{\cdot}CO_2^-$ was over 2-fold lower than that obtained in experiments without DMSO pretreatment.

Discussion

To our knowledge, this is the first study demonstrating free radical formation during acute formate poisoning. The evidence for formate-derived radical metabolites *in vivo* during acute sodium formate poisoning is provided by ESR spin trapping of the radicals from the metabolism of formate, which are detected in bile and urine as radical adducts. The use of [^{13}C]-sodium formate allowed an unambiguous assignment of the formate free radical metabolite as $^{\cdot}{}^{13}CO_2^-$, detected as its respective POBN/$^{\cdot}{}^{13}CO_2^-$ adduct. All of the control experiments showed that the radical adduct signals detected in bile of rats acutely treated by sodium formate were produced *in vivo* before sample collection and not *ex vivo* during sample collection.

Two non-free radical pathways have been proposed for the conversion of formate to carbon dioxide: oxidation through either the catalase-peroxidative system or the one-carbon pool. Many studies have shown that formate can be metabolized by the catalase-peroxidative system in *in vitro* preparations. Chance (26) showed that the catalase-peroxide compound I reacts with formate, and Aebi *et al.* (27) reported that formate oxidation by guinea pig liver was inhibited *in vitro* when animals were pretreated with AT, an inhibitor of catalase. A second pathway is metabolism via the folate-dependent one-carbon system. Formate enters this pool by combining with tetrahydrofolate (THF) to form formyl-THF, a reaction catalyzed by 10-formyl-THF synthetase (28). Various enzymatic reactions can direct the formyl-THF to other pathways, such as the Krebs' cycle, or to formyl THF/NADP oxidoreductase. 10-Formyl-THF can be oxidized to carbon dioxide with regeneration of THF through the enzyme formyl-THF dehydrogenase (29). Quantitative measurements by Chiao and Stokstad demonstrated that 75% of the formate oxidation in rats proceeds via 10-formyltetrahydrofolate synthase plus 10-formyltetrahydrofolate dehydrogenase, and about 25% occurs by a nonfolate, catalase-coupled reaction (30). From the ESR spin-trapping experiments presented in this paper, we suggest a free radical metabolic pathway in addition to that already known for the metabolism of formate.

Experiments with Desferal pretreatment indicate that free iron plays a role in the generation of POBN/$^{\cdot}{}^{13}CO_2^-$. The amplitude of the ESR signal from POBN/$^{\cdot}{}^{13}CO_2^-$ was decreased 2-fold by pretreatment with Desferal. A Fenton-like reaction will lead to the formation of the hydroxyl radical, which will, in turn, oxidize formate, forming the carbon dioxide anion radical.

$$H_2O_2 + Fe^{2+} \rightarrow {}^{\cdot}OH + Fe^{3+} + OH^- \quad [1]$$

$$HCO_2^- + {}^{\cdot}OH \rightarrow {}^{\cdot}CO_2^- + H_2O \quad [2]$$

Desferal has been shown to decrease hydroxyl radical generation in a model of iron overload (31). *In vitro*, both carbon dioxide anion radical and superoxide can release iron from ferritin (32). This reaction requires iron chelators, which are abundant *in vivo*, even including phospholipids (32). During acute formate poisoning, the formation of $^{\cdot}CO_2^-$ apparently caused the release of iron from ferritin, the main source of intracellular iron. Pretreatment with Desferal would be expected to decrease the amount of loosely bound iron originating from the reaction of reducing radicals with ferritin. Moreover, iron is a more efficient participant in the Fenton reaction at pH values associated with acidosis (33), which develops during formate intoxication. Thus, our finding that Desferal strongly inhibits radical generation by acute formate poisoning provides strong evidence for the role of iron-dependent hydroxyl radical generation.

In addition, the carbon dioxide anion radical reportedly can react directly with hydrogen peroxide with a rate constant of $k = 6 \times 10^5$ liter^{-1}·mol^{-1}·s^{-1} in an iron-independent reaction, which would not be inhibited by Desferal (34, 35):

$$\cdot CO_2^- + H_2O_2 \rightarrow CO_2 + \cdot OH + OH^- \quad [3]$$

In vivo, the most likely reaction of the carbon dioxide anion radical is with molecular oxygen, forming carbon dioxide and the superoxide radical.

$$\cdot CO_2^- + O_2 \rightarrow CO_2 + O_2^{\cdot -} \quad [4]$$

This reaction occurs with a diffusion-limited rate ($k = 4.2 \times 10^9$ liter $mol^{-1} \cdot s^{-1}$) (36). Disproportionation of this superoxide will form hydrogen peroxide, a necessary reactant in hydroxyl radical formation via the Fenton reaction.

$$2O_2^{\cdot -} + 2H^+ \rightarrow H_2O_2 + O_2 \quad [5]$$

The catalase suicide inhibitor AT was used to prevent hydrogen peroxide decomposition by catalase. There was a significant increase of the formate-derived radical formation when rats were pretreated with AT (Fig. 4*B*). This result supports the hypothesis that hydrogen peroxide reacts with iron in the Fenton reaction (reaction 1) to form the hydroxyl radical, which in turn oxidizes formate to the carbon dioxide anion radical. Alternatively, the inhibition of catalase by AT may increase the concentration of its substrate formate available for the one-electron oxidation pathway.

Hydrogen peroxide is normally present in cells in low concentrations. However, its concentration can increase when mitochondrial functions are impaired. It has been shown that formate inhibits cytochrome *c* oxidase, which may also lead to an increase in H_2O_2 (37).

One of the possible enzymatic sources of reactive oxygen species that may cause formate oxidation is the xanthine oxidase system. Xanthine oxidase is one of the major *in vivo* sources of the reactive oxygen species superoxide and hydrogen peroxide. Allopurinol, an inhibitor of xanthine oxidase (38), decreases superoxide production in xanthine oxidase-catalyzed reactions. Moreover, several reports have shown that allopurinol itself does not scavenge superoxide directly (39). We used allopurinol pretreatment, followed by formate and POBN administration, to reveal a possible role of this enzyme in radical formation. Statistically significant inhibition of radical formation was observed in rats pretreated with allopurinol, presumably by inhibiting hydrogen peroxide formation (Fig. 4*E*).

The finding that pretreatment of rats with 1-aminobenzotriazole decreased the ESR signal in rats treated with formate suggests that cytochrome P-450s, like xanthine oxidase, may promote formate oxidation by the formation of hydrogen peroxide (40).

The experiment with ^{13}C-labeled DMSO pretreatment supports the role of the Fenton reaction in the formate-derived radical formation. The methyl radical formed by the reaction of hydroxyl radical with DMSO shows that formate competes with DMSO for $\cdot OH$. Indeed, simulation of the spectrum showed that the relative concentration of POBN/$\cdot^{13}CO_2^-$ was over 2-fold lower than without DMSO pretreatment. Thus, we conclude that hydroxyl radical plays a role in the mechanism of free radical generation by formate.

Evidence for a key role of the *in vivo* Fenton reaction in free radical formation during acute formate poisoning was demonstrated in this ESR spin-trapping study. The results of this work may be important for understanding the pathogenesis not only of formate, but also of methanol poisoning because formic acid is a metabolic end product of methanol.

We are very grateful to Jean Corbett for help with animal care, Dr. Carolyn Mottley for the calculations of radical concentration, and Ms. Mary J. Mason for editorial assistance.

1. Liesivuori, J. & Savolainen, H. (1991) *Pharmacol. Toxicol.* **69,** 157–163.
2. Jacobsen, D. & McMartin, K. E. (1997) *J. Clin. Toxicol.* **35,** 127–143.
3. Clay, K. L., Murphy, R. C. & Watkins, W. D. (1975) *Toxicol. Appl. Pharmacol.* **34,** 49–61.
4. Liesivuori, J., Kosma, V.-M., Naukkarinen, A. & Savolainen, H. (1987) *Brit. J. Exp. Pathol.* **68,** 853–861.
5. Zitting, A., Savolainen, H. & Nickels, J. (1982) *Environ. Res.* **29,** 287–296.
6. McMartin, K. E., Makar, A. B., Martin, G., Palese, A. M. & Tephly, T. R. (1975) *Biochem. Med.* **13,** 319–333.
7. McMartin, K. E., Ambre, J. J. & Tephly, T. R. (1980) *Am. J. Med.* **68,** 414–418.
8. Jacobsen, D. & McMartin, K. E. (1986) *Med. Toxicol.* **1,** 309–334.
9. Erecinska, M. & Wilson, D. F. (1980) *Pharmacol. Ther.* **8,** 1–20.
10. Bralet, J., Bouvier, C., Schreiber, L. & Boquillon, M. (1991) *Brain Res.* **539,** 175–177.
11. Chacon, E. & Acosta, D. (1991) *Toxicol. Appl. Pharmacol*. **107,** 117–128.
12. Kadiiska, M. B., Hanna, P. M., Hernandez, L. & Mason, R. P. (1992) *Mol. Pharmacol*. **42,** 723–729.
13. Mugford, C. A., Mortillo, M., Mico, B. A. & Tarloff, J. B. (1992) *Fund. Appl. Toxicol.* **19,** 43–49.
14. Younis, H. S., Hoglen, N. C., Kuester, R. K., Gunawardhana, L. & Sipes, I. G. (2000) *Toxicol. Appl. Pharmacol*. **163,** 141–148.
15. Knecht, K. T., Thurman, R. G. & Mason, R. P. (1993) *Arch. Biochem. Biophys.* **303,** 339–348.
16. Rhoden, E. L., Pereira-Lima, L., Mauri, M., Lucas, M. L., Rhoden, C. R. & Bello-Klein, A. (1999) *Med. Sci. Res.* **27,** 829–830.
17. Mannering, G. J. & Parks, R. E. (1957) *Science* **126,** 1241–1242.
18. Tephly, T. R., Parks, R. E. & Mannering, G. J. (1964) *J. Pharmacol. Exp. Ther.* **143,** 292–300.
19. Committee on Care and Use of Laboratory Animals (1985) *Guide for the Care and Use of Laboratory Animals* (Natl. Inst. Health, Bethesda), DHHS Publ. No. (NIH) 85–23.
20. Duling, D. R. (1994) *J. Magn. Reson. Ser. B.* **104,** 105–110.
21. Weil, J. A., Bolton, J. R. & Wertz, J. E. (1994) in *Electron Paramagnetic Resonance: Elementary Theory and Practical Applications*, eds. Weil, J. A., Bolton, J. R. & Wertz, J. E. (Wiley, New York), pp. 492–519.
22. Kooser, R. G., Kirchman, E. & Matkov, T. (1992) *Concepts Magn. Reson.* **4,** 145–152.
23. Makino, K., Mossoba, M. M. & Riesz, P. (1983) *J. Phys. Chem.* **87,** 1369–1377.
24. Iwahashi, H., Deterding, L. J., Parker, C. E., Mason, R. P. & Tomer, K. B. (1996) *Free Radical Res.* **25,** 255–274.
25. Kadiiska, M. B., Burkitt, M. J., Xiang, Q.-H. & Mason, R. P. (1997) *Environ. Nutr. Interact.* **1,** 143–159.
26. Chance, B. (1950) *J. Biol. Chem.* **182,** 649–658.
27. Aebi, H., Frei, E., Knab, R. & Siegenthaler, P. (1957) *Helv. Physiol. Pharm. Acta* **15,** 150–167.
28. Whiteley, H. R. (1960) *Comp. Biochem Physiol.* **1,** 227–247.
29. Kutzbach, C. & Stokstad, E. L. R. (1968) *Biochem. Biophys. Res. Commun.* **30,** 111–117.
30. Chiao, F. & Stokstad, E. L. R. (1977) *Biochem. Biophys. Acta* **497,** 225–233.
31. Kadiiska, M. B., Burkitt, M. J., Xiang, Q.-H. & Mason, R. P. (1995) *J. Clin. Invest.* **96,** 1653–1657.
32. Reif, D. W., Schubert, J. & Aust, S. D. (1988) *Arch. Biochem. Biophys.* **264,** 238–243.
33. Schafer, F. Q. & Buettner, G. R. (2000) *Free Radical Biol. Med*. **28,** 1175–1181.
34. Schwarz, H. A. (1992) *J. Phys. Chem.* **96,** 8937–8941.
35. Kishore, K., Moorthy, P. N. & Rao, K. N. (1987) *Radiat. Phys. Chem.* **29,** 309–313.
36. Ilan, Y. & Rabani, J. (1976) *Int. J. Radiat. Phys. Chem.* **8,** 609–611.
37. Nicholls, P. (1976) *Biochem. Biophys. Acta* **430,** 13–29.
38. Massey, V., Komai, H. & Palmer, G. (1970) *J. Biol. Chem.* **245,** 2837–2844.
39. Klein, A. S., Joh, J. W., Rangan, U., Wang, D. & Bulkley, G. B. (1996) *Free Radical Biol. Med.* **21,** 713–717.
40. Goeptar, A. R., Scheerens, H. & Vermeulen, N. P. E. (1995) *Crit. Rev. Toxicol.* **25,** 25–65.